Acta Cryst. (1998). **B54**, 82–93

Temperature-Dependent Phase Transitions in Two Crystalline Host–Guest Complexes Derived from Mandelic Acid

Orm Hager,[a,b] Concepción Foces-Foces,[a]* Antonio L. Llamas-Saiz[a] and Edwin Weber[b]

[a]*Departamento de Cristalografía, Instituto de Química-Física 'Rocasolano', CSIC, Serrano 229, E-28006 Madrid, Spain, and* [b]*Institut für Organische Chemie, Technische Universität Bergakademie Freiberg, Leipziger Strasse 29, D-09596 Freiburg, Germany. E-mail: xconcha@iqfr.csic.es*

(Received 20 February 1997; accepted 23 July 1997)

Abstract

The supramolecular inclusion complexes of two mandelic acid-based chiral host compounds with dimethylformamide (DMF), (1) and (2), show reversible solid–solid state phase transitions upon lowering the temperature. For both inclusion complexes, the low- [(1*a*) and (2*a*) at 170 K] and the high- [(1*b*) at 250 and (2*b*) at 270 K] temperature structures were solved. (*R*)-1,1-Bis(4-*tert*-butylphenyl)-2-phenylethan-1,2-diol–dimethylformamide (1/1), $C_{28}H_{34}O_2.C_3H_7NO$ (1*a*), T = 170 K, monoclinic, $P2_1$, a = 14.4530 (14), b = 6.0540 (2), c = 16.1117 (14) Å, β = 105.332 (7)°, V = 1359.6 (2) Å^3, Z = 2, D_x = 1.162 g cm^{-3}; (1*b*), T = 250 K, monoclinic, $P2_1$, a = 24.8110 (20), b = 6.0739 (2), c = 18.8645 (10) Å, β = 98.100 (6)°, V = 2814.5 (3) Å^3, Z = 4, D_x = 1.123 g cm^{-3}. (*R*)-1,1-Bis(4-*tert*-butylphenyl)-2-(4-methylphenyl)ethan-1,2-diol–dimethylformamide (1/1), $C_{29}H_{36}O_2.C_3H_7NO$ (2*a*), T = 170 K, monoclinic, $P2_1$, a = 24.4457 (38), b = 5.9519 (6), c = 20.4609 (38) Å, β = 101.95 (1)°, V = 2912.5 (8) Å^3, Z = 4, D_x = 1.117 g cm^{-3}; (2*b*), T = 270 K, triclinic, $P1$, a = 14.4172 (28), b = 6.0303 (4), c = 17.5636 (56) Å, α = 88.74 (1), β = 101.43 (2), γ = 93.13 (1)°, V = 1494.4 (6) Å^3, Z = 2, D_x = 1.088 g cm^{-3}. The low-temperature forms have the higher crystallographic symmetry. In (1*b*) half of the DMF guests are twisted by 45.0° with respect to those in (1*a*). A comparative discussion of the four crystal packings is presented.

1. Introduction

A new class of chiral crystalline host compounds derived from natural mandelic acid has been previously synthesized, see (I) (Weber *et al.*, 1996, 1998*a*,*b*). These compounds present two hydroxyl groups, one being attached to the chiral center of the molecule, and three aromatic groups, one derived from mandelic acid. These host compounds were tested (Weber *et al.*, 1996, 1998*a*,*b*) with different solvents to obtain information on their inclusion behavior and on their possible usefulness in the separation of racemic mixtures by co-crystallization or vapor inclusion, as in the previously studied lactic acid derivatives (Weber *et al.*, 1992). In order to improve the selectivity of the inclusion, the efficiency of the enantiomer separation and the crystallization properties, we systematically introduced substituents to the chiral mandelic acid precursor [see (I)]. Two types of changes were considered: (1) increasing the bulkiness of the compound by introducing 'clathratogenic' groups (Weber & Wimmer, 1993) to encourage crystallization as host–guest complexes, and (2) introducing groups in strategic places to deliberately perturb the crystal packing, in order to promote the formation of host–guest networks. In the course of these studies we found a reversible phase transition of the crystalline inclusion compounds with dimethylformamide (DMF).

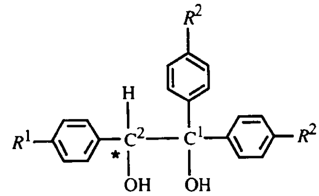

(I)

	R^1	R^2	Host	Guest
(1)	H	*tert*-butyl	*R*	DMF
(2)	Me	*tert*-butyl	*R*	DMF
(3)[a]	H	H	*R*	-
(4)[a]	H	H	*R,S*	-
(5)[a]	H	H	*R*	MeOH
(6)[b]	H	Me	*R*	-
(7)[b]	H	Me	*R*	MeOH
(8)[b]	H	*tert*-butyl	*R*	-
(9)[c]	Me	H	*R,S*	-
(10)[c]	Me	*tert*-butyl	*R*	DMSO
(11)[c]	Me	*tert*-butyl	*R,S*	DMSO

(*a*), (*b*) and (*c*) Weber *et al.* (1996, 1997*a*,*b*), respectively.

We report here the molecular and crystal structure of two DMF solvates at two temperatures, since both crystalline samples show temperature-dependent reversible solid-solid phase transitions. As pointed out by Dunitz (1995), a crystal can be described as a supramolecular unit, so any phase transition can be described as a supramolecular chemical reaction. A 'normal' reversible chemical reaction implies an equilibrium and can be reduced to an interaction between a few

ISSN 0108-7681 © 1998

molecules. The supramolecular reaction or phase transition, on the other hand, shows an extremely high level of cooperativity and shows no equilibrium in the sense that the chemical reaction in the gas or liquid state does.

For these studies we searched the October 1996 release of the Cambridge Structural Database (Allen *et al.*, 1991) for organic compounds which show a temperature-dependent phase transition and had reported structures of all the resulting forms. In a first search we retrieved 273 CSD entries corresponding to 187 compounds that contain the text string 'phase trans' either in the QUALifier, REMArks, PROPerties or CCOMment text fields. Secondly, we recovered 556 hits in the database, corresponding to every structure determination reported for each of the previous 187 compounds. There were only 65 cases where the crystal structure of more than one phase had been determined (a list of CSD refcodes is available from the authors on request). Accordingly, we believe that this type of analysis is very interesting, but scarce.

2. Experimental

2.1. *Synthesis*

The two host compounds (*R*)-1,1-bis(4-*tert*-butylphenyl)-2-phenylethan-1,2-diol and (*R*)-1,1-bis(4-*tert*-butylphenyl)-2-(4-methylphenyl)ethan-1,2-diol were synthesized as described previously (Weber *et al.*, 1998*a*,*b*).

2.2. *X-ray structure determination*

The relevant details of data collection and refinement procedure for the low- and high-temperature phases are given in Table 1. Single crystals were obtained by slow evaporation of a saturated solution of the corresponding host in DMF at room temperature. An Oxford Cryosystems Cryostream low-temperature device (Cosier & Glazer, 1986) was used for cooling the samples and during the process the unit-cell dimensions and the orientation matrix were monitored to check the stability of the crystal form. The phase transitions occur between 200 and 220 K for (1) and between 250 and 260 K for (2). The low- [(1*a*) and (2*a*)] and high- [(1*b*) and (2*b*)] temperature structures can be obtained reversibly by cycling the temperature back and forth, as was checked by looking at the diffraction patterns of the samples. However, the crystals broke and deteriorated after a few such cycles, therefore, several samples for each complex were used. Several attempts at data collection were performed with these samples largely because of the disorder found in the structures. In spite of all these efforts in selecting samples and temperature carefully, the final structures were not as precise as we would have wished (Table 1).

For the final data collection, the crystals were mounted according to the following methods: (*a*) at high temperature the samples were enclosed in Lindemann capillaries along with solvent to prevent decomposition, and (*b*) for the same reason, the crystals collected at low temperature were rapidly mounted at the end of a glass fiber and brought directly into the nitrogen gas stream of the cooling device at an initial temperature of 270 K. In order to stabilize the phases the low-temperature forms were kept at 170 K for ~1 d before starting data collection. As stated above, in the case of (1*a*) problems were found when the refinement was carried out and a new data set was therefore collected. With a new sample, a very slow cooling procedure was adopted, using steps of one degree without moving the goniometer head. After holding the crystal at the final temperature for 24 h to complete the phase transition, usable diffraction data could be obtained. Nonetheless, it shows a very high level of mosaicity that may be due to microruptures and the structure appears to be severely disordered.

The structures were solved by direct methods using *SIR*92 (Altomare *et al.*, 1994) and refined by full-matrix least squares procedures on *F* (*Xtal*3.2: Hall *et al.*, 1994). Empirical weighting schemes were obtained (Martínez-Ripoll & Cano, 1975). Most of the H atoms were located on difference-Fourier maps and the remaining ones [in (1*a*) and (2*b*)] were added in geometrically calculated positions. In (1*a*), (1*b*) and (2*b*) all hydrogen parameters were kept fixed, while in (2*a*) some were refined. The guest molecules in (1*a*), (1*b*) and (2*b*), the *tert*-butyl groups in (1*a*) and (1*b*) and the two phenyl rings bonded to C(1) in (1*a*) appeared disordered. The population parameters were only refined in (1*b*) because in the remaining forms the refinement became unstable, the population parameters being initially assigned from the isotropic displacement parameters. The absolute configuration of the host in (1) was given by the commercial optically pure mandelic acid precursor. Compound (2) was obtained from a racemic precursor; so its absolute configuration was assigned according to a previous structure determination of the same host molecule in a 1:1 complex with DMSO (Weber *et al.*, 1998*b*). Final atomic coordinates for non-H atoms are given in Table 2. Atomic scattering factors were taken from the *International Tables for X-ray Crystallography* (1974, Vol. IV).†

3. Results and discussion

3.1. *Molecular structure*

Some relevant intra- and intermolecular parameters are given in Table 3, according to the numbering scheme displayed in Fig. 1. The crystallographically independent host molecules in (1*b*), (2*a*) and (2*b*) display no

† Lists of atomic coordinates, anisotropic displacement parameters, complete geometry and structure factors have been deposited with the IUCr (Reference: BM0010). Copies may be obtained through The Managing Editor, International Union of Crystallography, 5 Abbey Square, Chester CH1 2HU, England.

Table 1. *Experimental details*

	(1*a*)	(1*b*)	(2*a*)	(2*b*)
Crystal data				
Chemical formula	$C_{28}H_{34}O_2.C_3H_7NO$	$C_{28}H_{34}O_2.C_3H_7NO$	$C_{29}H_{36}O_2.C_3H_7NO$	$C_{29}H_{36}O_2.C_3H_7NO$
Chemical formula weight	475.67	475.67	489.70	489.70
Cell setting	Monoclinic	Monoclinic	Monoclinic	Triclinic
Space group	$P2_1$	$P2_1$	$P2_1$	$P1$
a (Å)	14.4530 (14)	24.8110 (20)	24.4457 (38)	14.4172 (28)
b (Å)	6.0540 (2)	6.0739 (2)	5.9519 (6)	6.0303 (4)
c (Å)	16.1117 (14)	18.8645 (10)	20.4609 (38)	17.5636 (56)
α (°)				88.736 (10)
β (°)	105.332 (7)	98.100 (6)	101.954 (12)	101.43 (2)
γ (°)				93.135 (10)
V (Å^3)	1359.6 (2)	2814.5 (3)	2912.5 (8)	1494.4 (6)
Z	2	4	4	2
D_x (Mg m^{-3})	1.162	1.123	1.117	1.088
Radiation type	Cu $K\alpha$	Cu $K\alpha$	Cu $K\alpha$	Cu $K\alpha$
Wavelength (Å)	1.5418	1.5418	1.5418	1.5418
No. of reflections for cell parameters	66	81	42	69
θ range (°)	2–45	2–45	2–45	2–45
μ (mm^{-1})	0.5735	0.5541	0.5480	0.5340
Temperature (K)	170	250	170	270
Crystal form	Prism	Prism	Prism	Prism
Crystal size (mm)	0.50 × 0.33 × 0.26	0.70 × 0.30 × 0.30	0.80 × 0.41 × 0.41	0.40 × 0.33 × 0.20
Crystal color	Colorless	Colorless	Colorless	Colorless
Data collection				
Diffractometer	Philips PW1100	Philips PW1100	Philips PW1100	Philips PW1100
Data collection method	$\omega/2\theta$ scans	$\omega/2\theta$ scans	$\omega/2\theta$ scans	$\omega/2\theta$ scans
Absorption correction	None	None	None	None
No. of measured reflections	2598	5444	5596	4980
No. of independent reflections	2506	5295	5457	4980
No. of observed reflections	1844	3123	4500	3474
Criterion for observed reflections	$I > 2\sigma(I)$	$I > 2\sigma(I)$	$I > 2\sigma(I)$	$I > 2\sigma(I)$
R_{int}	0.022	0.006	0.042	–
θ_{max} (°)	64.88	65.12	65.24	64.36
Range of h, k, l	$-16 \rightarrow h \rightarrow 0$ $-7 \rightarrow k \rightarrow 0$ $-18 \rightarrow l \rightarrow 18$	$-29 \rightarrow h \rightarrow 28$ $0 \rightarrow k \rightarrow 7$ $0 \rightarrow l \rightarrow 22$	$-28 \rightarrow h \rightarrow 28$ $0 \rightarrow k \rightarrow 7$ $0 \rightarrow l \rightarrow 24$	$-16 \rightarrow h \rightarrow 16$ $0 \rightarrow k \rightarrow 7$ $-20 \rightarrow l \rightarrow 20$
No. of standard reflections	2	2	2	2
Frequency of standard reflections (min)	90	90	90	90
Intensity decay (%)	None	None	None	None
Refinement				
Refinement on	F	F	F	F
R	0.052	0.080	0.054	0.071
wR	0.057	0.101	0.063	0.083
S	1.085	0.900	1.023	0.952
No. of reflections used in refinement	1844	3123	4500	3474
No. of parameters used	486	639	941	664
No. of restraints	46	0	0	0
Degrees of freedom	1404	2484	3559	2810
Ratio of freedom	4.2	4.9	4.8	5.2
H-atom treatment	H-atom parameters not refined	H-atom parameters not refined	Mixed	H-atom parameters not refined
Weighting scheme	Empirical to give no trends in <$w\Delta F^2$> *versus* <$\lvert F_{obs}\rvert$> and <$\sin\theta/\lambda$>	Empirical to give no trends in <$w\Delta F^2$> *versus* <$\lvert F_{obs}\rvert$> and <$\sin\theta/\lambda$>	Empirical to give no trends in <$w\Delta F^2$> *versus* <$\lvert F_{obs}\rvert$> and <$\sin\theta/\lambda$>	Empirical to give no trends in <$w\Delta F^2$> *versus* <$\lvert F_{obs}\rvert$> and <$\sin\theta/\lambda$>
Δ/σ_{max}	0.569	0.088	1.056	2.601
$\Delta\rho_{max}$ (e Å^{-3})	0.195	0.431	0.320	0.532
$\Delta\rho_{min}$ (e Å^{-3})	−0.217	−0.465	−0.275	−0.252
Extinction method	None	Zachariasen (1968)	Zachariasen (1968)	Zachariasen (1968)
Extinction coefficient	–	7822.573	2588.270	5256.552

Table 1 (*cont.*)

	(1*a*)	(1*b*)	(2*a*)	(2*b*)
Source of atomic scattering factors	*International Tables for X-ray Crystallography* (1974, Vol. IV)	*International Tables for X-ray Crystallography* (1974, Vol. IV)	*International Tables for X-ray Crystallography* (1974, Vol. IV)	*International Tables for X-ray Crystallography* (1974, Vol. IV)
Absolute configuration	Known by synthesis	Known by synthesis	The absolute configuration was assigned to agree with the known chirality at C2 obtained from a previous determination (Weber *et al.*, 1998*b*)	The absolute configuration was assigned to agree with the known chirality at C2 obtained from a previous determination (Weber *et al.*, 1998*b*)
Computer programs				
Data collection	Philips PW1100	Philips PW1100	Philips PW1100	Philips PW1100
Cell refinement	*LSUCRE* (Appleman, 1984)	*LSUCRE* (Appleman, 1984)	*LSUCRE* (Appleman, 1984)	*LSUCRE* (Appleman, 1984)
Data reduction	*Xtal DIFDAT SORTRF ADDREF* (Hall *et al.*, 1994)	*Xtal DIFDAT SORTRF ADDREF* (Hall *et al.*, 1994)	*Xtal DIFDAT SORTRF ADDREF* (Hall *et al.*, 1994)	*Xtal DIFDAT SORTRF ADDREF* (Hall *et al.*, 1994)
Structure solution	*SIR*92 (Altomare *et al.*, 1994)	*SIR*92 (Altomare *et al.*, 1994)	*SIR*92 (Altomare *et al.*, 1994)	*SIR*92 (Altomare *et al.*, 1994)
Structure refinement	*Xtal CRYLSQ* (Hall *et al.*, 1994)	*Xtal CRYLSQ* (Hall *et al.*, 1994)	*Xtal CRYLSQ* (Hall *et al.*, 1994)	*Xtal CRYLSQ* (Hall *et al.*, 1994)
Preparation of material for publication	*Xtal BONDLA CIFIO* (Hall *et al.*, 1994)	*Xtal BONDLA CIFIO* (Hall *et al.*, 1994)	*Xtal BONDLA CIFIO* (Hall *et al.*, 1994)	*Xtal BONDLA CIFIO* (Hall *et al.*, 1994)

significant differences in terms of bond distances and angles, as shown by half normal probability plots (Nardelli, 1983); the main differences are due to the *tert*-butyl group conformation and the torsion angle of the C(21)–C(26) phenyl ring in molecule 2 of (2*a*). Apart from the twist of the phenyl rings at C(1), the observed geometries compare well with those of the previously reported analogous compounds [see (I) (Weber *et al.*, 1996, 1998*a*,*b*)]. These are: angular distortion at C(1) and C(11) as a consequence of the almost staggered situation of the C(11)–C(16) phenyl ring with respect to the C(1)—C(2) bond; hydroxyl groups in *gauche* conformation; phenyl angular distortions at *para* positions due to the *tert*-butyl and methyl groups that close the *ipso* angle (Domenicano & Murray-Rust, 1979).

The DMF guest molecules were found to be disordered in (1*a*), (1*b*) and (2*b*). The N atom has pyramidal character with the Me groups adopting two different positions with respect to the C(3)—N(1) bond: one Me group and the N-atom lone pair interchange their positions while the others remain unchanged. These guest molecules present two orientations with respect to the host, as measured by the N(1)—C(3)—O(6)···O(4) pseudo-torsion angle (Table 3); one orientation is in (1*a*) and guest 2 in (1*b*), and the other one by the remaining guest molecules.

3.2. *Hydrogen-bonding pattern*

In all compounds (Fig. 2), a constant feature of the crystal packing is the chains formed by host molecules linked through the DMF along the crystallographic **b** axis. The guest molecule acts as an acceptor of two O—H···O hydrogen bonds, from two different host molecules, which are the primary interactions. The weaker secondary interactions (C—H···O and C—H···π phenyl electron cloud; Table 3) are also not so well preserved in all four structures, as we will see later. The differences found in the secondary interactions seem to be directly related to the structural changes observed after the phase transition. The primary subunits, *i.e.* the O—H···O hydrogen-bonded chains, are, however, preserved.

3.3. *Structural comparison between the forms of (1)*

The two independent host molecules in (1*b*), Fig. 3(*b*), are related by a pseudo-twofold screw axis parallel to **b**, located at x = 0.249 (4), z = 0.235 (4) and with a translation of 0.46 (2) fractional units [χ^2 values for x, y and z are 42.8, 5.8 and 3.7 *versus* the tabulated one of 33.9, H atoms and *tert*-butyl groups excluded (Nardelli, 1983)]. The unit cell of (1*b*) (**a**′, **b**′, **c**′) is double the volume of that of (1*a*) (**a**, **b**, **c**) and is related to it as follows: **a**′ = **a** − **c**, **b**′ = **b** and **c**′ = **a** + **c**, with an origin shift of ($-\frac{1}{2}$, 0, $\frac{1}{2}$), Figs. 3(*a*) and 3(*b*) (calculated unit cell values: 24.323, 6.054, 18.583 Å, β = 96.440°, see Table 1). When crystal symmetry is compared, every second 2_1 screw axis disappears after the phase transition from (1*a*) to (1*b*), *i.e.* that located at (0, y, $\frac{1}{2}$) in (1*a*) and all symmetry-equivalent ones.

The phase transition can be described from a structural point of view as a rearrangement of crystal domains, *i.e.* a 'displacive type' (McCrone, 1965). These domains are formed by two layers of host molecules located at x = 1/4 and 3/4 approximately and parallel to the **bc** plane in (1*b*), Fig. 3(*b*). Between these two layers there are

Table 2. *Fractional atomic coordiantes and equivalent isotropic displacement parameters (Å^2)*

$U_{eq} = (1/3)\Sigma_i\Sigma_j a_i^* a_j^* \mathbf{a}_i.\mathbf{a}_j$.

	x	*y*	*z*	U_{eq}
(1*a*)				
N1	−0.1113 (3)	0.8182 (12)	0.8638 (3)	0.062 (3)
O6	0.0478 (2)	0.8515 (11)	0.9280 (3)	0.071 (2)
C3	−0.0256 (4)	0.7413 (13)	0.9022 (4)	0.063 (3)
C8	−0.1236 (18)	1.040 (7)	0.825 (2)	0.110 (17)
C8*A*	−0.1274 (11)	1.054 (3)	0.8728 (10)	0.065 (7)
C9	−0.1934 (4)	0.6766 (15)	0.8368 (5)	0.081 (4)
C1	0.1835 (3)	0.40000	0.8162 (3)	0.042 (2)
C2	0.1954 (3)	0.2477 (12)	0.8957 (3)	0.043 (2)
C31	0.2876 (3)	0.2842 (13)	0.9653 (3)	0.047 (3)
C32	0.3536 (4)	0.1122 (15)	0.9849 (3)	0.064 (3)
C33	0.4385 (5)	0.145 (2)	1.0500 (4)	0.091 (5)
C34	0.4571 (5)	0.337 (2)	1.0933 (4)	0.097 (5)
C35	0.3926 (5)	0.5031 (17)	1.0745 (4)	0.086 (4)
C36	0.3076 (4)	0.4772 (14)	1.0104 (3)	0.065 (3)
O4	0.1797 (2)	0.6257 (10)	0.84223 (18)	0.0403 (16)
O5	0.1145 (2)	0.2869 (10)	0.9298 (2)	0.056 (2)
C11	0.0904 (3)	0.3406 (12)	0.7469 (3)	0.049 (3)
C12	0.0458 (6)	0.1158 (18)	0.7432 (5)	0.038 (5)
C13	−0.0375 (5)	0.0688 (16)	0.6786 (5)	0.036 (5)
C14	−0.0822 (11)	0.229 (3)	0.6188 (10)	0.045 (7)
C15	−0.0413 (12)	0.439 (3)	0.6263 (12)	0.052 (10)
C16	0.0402 (13)	0.495 (3)	0.6905 (10)	0.050 (9)
C12*A*	0.0832 (7)	0.151 (2)	0.7034 (7)	0.063 (7)
C13*A*	0.0046 (7)	0.106 (2)	0.6336 (7)	0.069 (7)
C14*A*	−0.0670 (12)	0.262 (3)	0.6046 (11)	0.052 (9)
C15*A*	−0.0534 (13)	0.463 (3)	0.6466 (11)	0.036 (7)
C16*A*	0.0274 (12)	0.507 (3)	0.7134 (9)	0.031 (6)
C17	−0.1717 (11)	0.169 (3)	0.5509 (9)	0.049 (8)
C18	−0.1385 (12)	0.044 (4)	0.4836 (11)	0.074 (11)
C19	−0.2368 (7)	0.014 (3)	0.5857 (9)	0.082 (8)
C20	−0.2311 (13)	0.378 (4)	0.5201 (18)	0.102 (13)
C17*A*	−0.1568 (10)	0.213 (2)	0.5242 (8)	0.038 (6)
C18*A*	−0.2485 (12)	0.285 (4)	0.5450 (18)	0.101 (15)
C19*A*	−0.1428 (8)	0.340 (2)	0.4479 (6)	0.061 (6)
C20*A*	−0.1683 (11)	−0.033 (3)	0.5001 (13)	0.070 (10)
C21	0.2686 (3)	0.3825 (14)	0.7784 (3)	0.046 (3)
C22	0.2785 (6)	0.1562 (19)	0.7428 (6)	0.042 (4)
C23	0.3552 (6)	0.122 (2)	0.7061 (6)	0.043 (4)
C24	0.4208 (8)	0.299 (3)	0.7066 (8)	0.033 (6)
C25	0.4056 (9)	0.491 (2)	0.7425 (7)	0.043 (6)
C26	0.3288 (7)	0.522 (2)	0.7788 (6)	0.042 (5)
C22*A*	0.3292 (9)	0.231 (2)	0.7763 (8)	0.038 (6)
C23*A*	0.4067 (12)	0.232 (3)	0.7382 (13)	0.046 (9)
C24*A*	0.4361 (10)	0.427 (4)	0.7064 (11)	0.038 (8)
C25*A*	0.3790 (8)	0.610 (3)	0.7059 (9)	0.041 (6)
C26*A*	0.3001 (8)	0.606 (2)	0.7400 (9)	0.040 (6)
C27	0.5005 (6)	0.266 (2)	0.6596 (6)	0.037 (5)
C28	0.4644 (11)	0.344 (4)	0.5672 (11)	0.067 (9)
C29	0.5874 (10)	0.404 (3)	0.7052 (11)	0.053 (9)
C30	0.5357 (6)	0.0289 (18)	0.6621 (5)	0.043 (4)
C27*A*	0.5241 (12)	0.427 (3)	0.6713 (8)	0.045 (8)
C28*A*	0.5012 (11)	0.306 (4)	0.5878 (16)	0.051 (11)
C29*A*	0.6123 (13)	0.332 (4)	0.7380 (12)	0.051 (10)
C30*A*	0.5534 (9)	0.666 (3)	0.6543 (12)	0.073 (9)
(1*b*), molecule 1				
N101	0.0080 (3)	0.641 (3)	0.3732 (5)	0.089 (6)
O106	0.0617 (3)	0.851 (2)	0.4492 (5)	0.103 (5)
C103	0.0249 (4)	0.725 (2)	0.4341 (6)	0.072 (6)
C108	0.0459 (12)	0.600 (9)	0.3157 (18)	0.10 (2)
C108*A*	0.0247 (17)	0.755 (8)	0.3087 (16)	0.13 (3)
C109	−0.0353 (6)	0.475 (3)	0.3609 (9)	0.119 (10)
C101	0.1832 (3)	0.40000	0.4760 (4)	0.047 (4)
C102	0.1476 (3)	0.2560 (18)	0.5168 (5)	0.052 (4)
C131	0.1541 (3)	0.302 (2)	0.5966 (4)	0.053 (4)
C132	0.1811 (4)	0.149 (2)	0.6438 (5)	0.070 (5)
C133	0.1881 (4)	0.188 (3)	0.7172 (6)	0.089 (7)
C134	0.1675 (5)	0.380 (3)	0.7422 (5)	0.088 (7)
C135	0.1405 (7)	0.527 (3)	0.6979 (6)	0.099 (8)
C136	0.1330 (5)	0.484 (3)	0.6238 (6)	0.090 (7)
O104	0.1693 (2)	0.6301 (16)	0.4851 (3)	0.050(3)
O105	0.0914 (2)	0.2914 (16)	0.4873 (3)	0.061 (3)
C111	0.1748 (3)	0.350 (2)	0.3946 (4)	0.050 (4)
C112	0.1595 (4)	0.147 (2)	0.3660 (5)	0.065 (5)
C113	0.1542 (4)	0.108 (2)	0.2940 (5)	0.062 (5)
C114	0.1652 (3)	0.264 (2)	0.2461 (4)	0.055 (4)
C115	0.1823 (4)	0.470 (2)	0.2755 (4)	0.067 (5)
C116	0.1875 (5)	0.507 (2)	0.3476 (5)	0.073 (6)
C117	0.1585 (4)	0.229 (2)	0.1653 (5)	0.063 (5)
C118	0.1036 (6)	0.302 (4)	0.1325 (6)	0.124 (10)
C119	0.2002 (7)	0.367 (3)	0.1301 (7)	0.107 (9)
C120	0.1701 (7)	−0.009 (3)	0.1454 (6)	0.100 (8)
C121	0.2429 (3)	0.374 (2)	0.5059 (4)	0.045 (4)
C122	0.2691 (3)	0.178 (2)	0.4976 (5)	0.065 (5)
C123	0.3238 (4)	0.153 (2)	0.5245 (5)	0.066 (5)
C124	0.3549 (3)	0.322 (2)	0.5581 (4)	0.048 (4)
C125	0.3275 (3)	0.517 (2)	0.5649 (6)	0.067 (5)
C126	0.2725 (4)	0.542 (2)	0.5399 (5)	0.063 (5)
C127	0.4160 (3)	0.297 (2)	0.5835 (5)	0.064 (5)
C128	0.4461 (4)	0.394 (3)	0.5248 (7)	0.091 (7)
C129	0.4333 (4)	0.428 (3)	0.6521 (6)	0.087 (7)
C130	0.4322 (4)	0.061 (2)	0.5944 (8)	0.091 (7)
(1*b*), molecule 2				
N201	0.4878 (3)	0.345 (2)	0.1204 (6)	0.085 (6)
O206	0.4373 (3)	0.383 (2)	0.0130 (5)	0.094 (5)
C203	0.4613 (5)	0.267 (3)	0.0604 (8)	0.098 (8)
C208	0.4951 (7)	0.581 (3)	0.1304 (10)	0.127 (11)
C209	0.5170 (8)	0.202 (4)	0.1707 (12)	0.154 (14)
C201	0.3169 (3)	−0.0561 (18)	−0.0080 (4)	0.047 (4)
C202	0.3480 (3)	−0.212 (2)	−0.0539 (4)	0.055 (4)
C231	0.3351 (3)	−0.179 (2)	−0.1330 (5)	0.057 (5)
C232	0.3091 (4)	−0.346 (2)	−0.1758 (6)	0.070 (6)
C233	0.2967 (5)	−0.317 (3)	−0.2506 (6)	0.088 (7)
C234	0.3100 (5)	−0.128 (3)	−0.2816 (6)	0.079 (7)
C235	0.3342 (5)	0.038 (2)	−0.2404 (7)	0.086 (7)
C236	0.3482 (4)	0.011 (2)	−0.1667 (5)	0.071 (6)
O204	0.3309 (2)	0.1679 (16)	−0.0214 (3)	0.056 (3)
O205	0.4046 (2)	−0.1763 (16)	−0.0322 (3)	0.061 (3)
C211	0.3307 (3)	−0.108 (2)	0.0706 (4)	0.049 (4)
C212	0.3404 (5)	−0.314 (2)	0.0993 (5)	0.075 (6)
C213	0.3492 (6)	−0.354 (3)	0.1715 (6)	0.091 (7)
C214	0.3481 (4)	−0.190 (2)	0.2215 (5)	0.067 (5)
C215	0.3383 (7)	0.018 (2)	0.1932 (6)	0.108 (9)
C216	0.3303 (6)	0.058 (2)	0.1202 (6)	0.093 (8)
C217	0.3549 (5)	−0.227 (3)	0.3026 (5)	0.088 (7)
C218	0.4043 (7)	−0.105 (5)	0.3382 (8)	0.121 (13)
C219	0.3065 (8)	−0.100 (4)	0.3354 (8)	0.095 (10)
C220	0.3463 (11)	−0.468 (3)	0.3228 (9)	0.114 (13)
C218*A*	0.31380	−0.36310	0.32370	0.10400
C219*A*	0.40310	−0.32930	0.32320	0.07900
C220*A*	0.35560	−0.03200	0.33590	0.08400
C221	0.2557 (3)	−0.077 (2)	−0.0310 (4)	0.049 (4)
C222	0.2285 (4)	−0.272 (2)	−0.0225 (5)	0.062 (5)
C223	0.1732 (3)	−0.294 (2)	−0.0413 (5)	0.063 (5)
C224	0.1414 (3)	−0.115 (2)	−0.0698 (4)	0.055 (4)
C225	0.1689 (4)	0.078 (2)	−0.0789 (5)	0.066 (5)
C226	0.2245 (3)	0.100 (2)	−0.0613 (5)	0.060 (5)
C227	0.0798 (3)	−0.138 (2)	−0.0890 (4)	0.058 (5)
C228	0.0677 (5)	−0.278 (3)	−0.1564 (7)	0.107 (9)

Table 2 (*cont.*)

	x	y	z	U_{eq}
C229	0.0548 (4)	−0.238 (3)	−0.0278 (6)	0.105 (9)
C230	0.0517 (4)	0.085 (3)	−0.1044 (8)	0.093 (7)
(2*a*), molecule 1				
N101	0.00113 (15)	0.6099 (13)	0.3741 (2)	0.058 (2)
O106	0.05710 (15)	0.8538 (11)	0.4410 (3)	0.072 (2)
C103	0.0175 (2)	0.7202 (13)	0.4291 (3)	0.055 (3)
C108	0.0317 (3)	0.620 (3)	0.3207 (4)	0.108 (6)
C109	−0.0428 (3)	0.4427 (18)	0.3689 (6)	0.087 (5)
C101	0.18235 (15)	0.40000	0.4696 (2)	0.0279 (18)
C102	0.14616 (15)	0.2454 (11)	0.5045 (2)	0.030 (2)
C131	0.15740 (16)	0.2737 (11)	0.5802 (2)	0.036 (2)
C132	0.1846 (2)	0.1076 (13)	0.6196 (2)	0.047 (3)
C133	0.1955 (2)	0.1279 (17)	0.6892 (3)	0.060 (3)
C134	0.1788 (2)	0.3163 (15)	0.7196 (2)	0.058 (3)
C135	0.1503 (3)	0.4806 (15)	0.6787 (3)	0.066 (3)
C136	0.1394 (3)	0.4593 (13)	0.6097 (3)	0.052 (3)
C137	0.1902 (4)	0.331 (2)	0.7947 (3)	0.083 (6)
O104	0.16900 (11)	0.6288 (9)	0.47917 (14)	0.0328 (14)
O105	0.08856 (11)	0.2950 (10)	0.47587 (15)	0.0390 (16)
C111	0.17280 (14)	0.3524 (11)	0.39375 (19)	0.0299 (18)
C112	0.15159 (17)	0.1506 (12)	0.3652 (2)	0.038 (2)
C113	0.14326 (18)	0.1197 (12)	0.2958 (2)	0.042 (2)
C114	0.15569 (17)	0.2835 (12)	0.2540 (2)	0.039 (2)
C115	0.1779 (2)	0.4811 (12)	0.2827 (2)	0.043 (2)
C116	0.18657 (17)	0.5167 (12)	0.3521 (2)	0.036 (2)
C117	0.1447 (2)	0.2392 (13)	0.1779 (2)	0.053 (3)
C118	0.1829 (2)	0.0535 (14)	0.1625 (3)	0.058 (3)
C119	0.0853 (3)	0.167 (3)	0.1530 (4)	0.116 (7)
C120	0.1597 (5)	0.4469 (16)	0.1385 (3)	0.100 (5)
C121	0.24394 (15)	0.3669 (11)	0.50118 (19)	0.0282 (18)
C122	0.26923 (16)	0.1606 (11)	0.4957 (2)	0.031 (2)
C123	0.32607 (15)	0.1271 (11)	0.5242 (2)	0.033 (2)
C124	0.35874 (15)	0.2992 (11)	0.5568 (2)	0.0309 (19)
C125	0.33277 (17)	0.5032 (12)	0.5620 (2)	0.042 (2)
C126	0.27588 (17)	0.5359 (12)	0.5352 (2)	0.039 (2)
C127	0.42239 (16)	0.2752 (11)	0.5838 (2)	0.036 (2)
C128	0.45248 (17)	0.4042 (13)	0.5361 (2)	0.044 (2)
C129	0.43871 (19)	0.3723 (13)	0.6545 (2)	0.045 (3)
C130	0.4410 (2)	0.0326 (12)	0.5853 (3)	0.047 (3)
(2*a*), molecule 2				
N201	0.49918 (15)	0.3213 (11)	0.1307 (2)	0.050 (2)
O206	0.44678 (15)	0.5703 (11)	0.0616 (3)	0.072 (2)
C203	0.48163 (18)	0.4188 (13)	0.0729 (3)	0.052 (3)
C208	0.4777 (3)	0.388 (2)	0.1895 (4)	0.090 (5)
C209	0.5356 (3)	0.1285 (17)	0.1361 (5)	0.085 (4)
C201	0.32409 (15)	0.1317 (11)	0.02756 (18)	0.0292 (18)
C202	0.35948 (15)	−0.0413 (10)	−0.0017 (2)	0.029 (2)
C231	0.34807 (15)	−0.0461 (11)	−0.0781 (2)	0.032 (2)
C232	0.31976 (17)	−0.2237 (12)	−0.1129 (2)	0.040 (2)
C233	0.3127 (2)	−0.2372 (13)	−0.1826 (2)	0.046 (3)
C234	0.33357 (18)	−0.0695 (13)	−0.2181 (2)	0.046 (2)
C235	0.3604 (2)	0.1080 (13)	−0.1834 (2)	0.051 (3)
C236	0.3681 (2)	0.1235 (13)	−0.1142 (2)	0.043 (2)
C237	0.3287 (3)	−0.0914 (17)	−0.2929 (3)	0.063 (3)
O204	0.33608 (11)	0.3539 (9)	0.00736 (14)	0.0308 (13)
O205	0.41676 (11)	0.0083 (9)	0.02414 (15)	0.0364 (15)
C211	0.33545 (15)	0.1223 (11)	0.10455 (19)	0.0301 (18)
C212	0.35552 (18)	−0.0664 (11)	0.1418 (2)	0.036 (2)
C213	0.36084 (18)	−0.0693 (11)	0.2108 (2)	0.038 (2)
C214	0.34624 (15)	0.1156 (11)	0.2455 (2)	0.0325 (19)
C215	0.32703 (17)	0.3032 (11)	0.2081 (2)	0.035 (2)
C216	0.32166 (16)	0.3055 (11)	0.1386 (2)	0.033 (2)
C217	0.34848 (16)	0.1013 (11)	0.3212 (2)	0.034 (2)
C218	0.3006 (2)	−0.0535 (12)	0.3324 (2)	0.042 (2)
C219	0.4042 (2)	0.0025 (14)	0.3572 (2)	0.049 (3)
C220	0.3412 (2)	0.3293 (13)	0.3515 (2)	0.048 (3)

Table 2 (*cont.*)

	x	y	z	U_{eq}
C221	0.26212 (15)	0.0879 (11)	0.00185 (18)	0.0289 (18)
C222	0.23920 (16)	−0.1211 (11)	0.0098 (2)	0.034 (2)
C223	0.18246 (16)	−0.1633 (11)	−0.0139 (2)	0.036 (2)
C224	0.14621 (16)	0.0003 (11)	−0.0452 (2)	0.033 (2)
C225	0.16928 (16)	0.2112 (10)	−0.0510 (2)	0.032 (2)
C226	0.22627 (16)	0.2547 (11)	−0.0288 (2)	0.032 (2)
C227	0.08478 (16)	−0.0532 (11)	−0.0749 (2)	0.038 (2)
C228	0.0825 (2)	−0.1845 (15)	−0.1402 (3)	0.054 (3)
C229	0.0602 (2)	−0.2022 (14)	−0.0270 (3)	0.054 (3)
C230	0.0496 (2)	0.1552 (14)	−0.0896 (5)	0.074 (4)
(2*b*), molecule 1				
N101	−0.1333 (9)	0.585 (2)	0.8710 (8)	0.112 (7)
O106	−0.0095 (8)	0.8272 (19)	0.8858 (7)	0.135 (7)
C103	−0.0578 (11)	0.684 (2)	0.9095 (8)	0.105 (8)
C108	−0.155 (3)	0.582 (9)	0.788 (3)	0.16 (3)
C108*A*	−0.181 (5)	0.700 (11)	0.804 (2)	0.21 (4)
C109	−0.1787 (15)	0.407 (3)	0.9036 (15)	0.178 (16)
C101	0.14056	0.40000	0.78721	0.046 (3)
C102	0.1434 (6)	0.2397 (14)	0.8570 (5)	0.050 (3)
C131	0.2304 (7)	0.2692 (15)	0.9208 (5)	0.051 (3)
C132	0.2979 (7)	0.115 (2)	0.9327 (6)	0.076 (5)
C133	0.3759 (8)	0.137 (2)	0.9959 (7)	0.093 (6)
C134	0.3852 (8)	0.307 (2)	1.0456 (6)	0.084 (6)
C135	0.3181 (9)	0.464 (2)	1.0338 (7)	0.091 (6)
C136	0.2406 (8)	0.4464 (18)	0.9725 (6)	0.072 (5)
C137	0.4668 (10)	0.322 (3)	1.1162 (7)	0.128 (9)
O104	0.1369 (5)	0.6257 (13)	0.8130 (4)	0.052 (2)
O105	0.0604 (6)	0.2699 (13)	0.8879 (5)	0.062 (3)
C111	0.0545 (6)	0.3465 (15)	0.7228 (5)	0.047 (3)
C112	0.0113 (8)	0.1390 (17)	0.7103 (6)	0.081 (5)
C113	−0.0645 (8)	0.0945 (17)	0.6488 (6)	0.078 (5)
C114	−0.0986 (7)	0.2599 (17)	0.5962 (6)	0.064 (4)
C115	−0.0560 (9)	0.4642 (18)	0.6099 (7)	0.088 (6)
C116	0.0191 (7)	0.5114 (17)	0.6715 (6)	0.071 (4)
C117	−0.1799 (8)	0.216 (2)	0.5280 (7)	0.091 (6)
C118	−0.2635 (9)	0.323 (3)	0.5380 (9)	0.139 (10)
C119	−0.1553 (12)	0.348 (3)	0.4521 (7)	0.117 (8)
C120	−0.1884 (12)	−0.014 (3)	0.5014 (11)	0.161 (11)
C121	0.2296 (6)	0.3933 (15)	0.7535 (5)	0.044 (3)
C122	0.2510 (7)	0.1976 (16)	0.7208 (6)	0.062 (4)
C123	0.3306 (7)	0.1869 (16)	0.6897 (6)	0.061 (4)
C124	0.3936 (7)	0.3725 (16)	0.6878 (5)	0.053 (4)
C125	0.3702 (6)	0.5661 (15)	0.7180 (5)	0.052 (4)
C126	0.2921 (7)	0.5753 (15)	0.7512 (5)	0.055 (4)
C127	0.4826 (7)	0.3564 (15)	0.6542 (6)	0.058 (4)
C128	0.5531 (9)	0.218 (3)	0.7124 (8)	0.109 (8)
C129	0.4609 (9)	0.224 (2)	0.5775 (8)	0.107 (7)
C130	0.5300 (11)	0.578 (2)	0.6406 (10)	0.124 (9)
(2*b*), molecule 2				
N201	0.1262 (7)	1.1032 (18)	0.1297 (6)	0.089 (5)
O206	0.0088 (8)	1.3359 (18)	0.1136 (7)	0.120 (6)
C203	0.0559 (9)	1.209 (2)	0.0884 (7)	0.086 (6)
C208	0.1537 (13)	1.129 (4)	0.2118 (12)	0.185 (16)
C209	0.167 (3)	0.937 (7)	0.099 (3)	0.15 (3)
C209*A*	0.181 (5)	0.940 (8)	0.097 (4)	0.15 (3)
C201	−0.1509 (6)	0.8560 (15)	0.2069 (5)	0.048 (3)
C202	−0.1510 (6)	0.7046 (15)	0.1366 (5)	0.053 (4)
C231	−0.2362 (7)	0.7257 (16)	0.0724 (5)	0.054 (4)
C232	−0.3037 (9)	0.551 (2)	0.0593 (6)	0.088 (6)
C233	−0.3842 (9)	0.570 (3)	−0.0011 (7)	0.117 (8)
C234	−0.3978 (9)	0.748 (3)	−0.0481 (6)	0.095 (7)
C235	−0.3291 (12)	0.917 (2)	− 0.0348(7)	0.113 (8)
C236	−0.2495 (9)	0.9050 (19)	0.0244 (6)	0.087 (5)
C237	−0.4842 (12)	0.758 (4)	−0.1125 (8)	0.155 (12)
O204	−0.1439 (5)	1.0840 (13)	0.1819 (4)	0.052 (2)
O205	−0.0671 (6)	0.7609 (14)	0.1074 (5)	0.064 (3)

Table 2 (*cont.*)

	x	y	z	U_{eq}
C211	−0.0655 (6)	0.8168 (15)	0.2738 (5)	0.048 (3)
C212	−0.0188 (7)	0.6204 (16)	0.2839 (6)	0.063 (4)
C213	0.0536 (8)	0.5890 (17)	0.3476 (6)	0.071 (5)
C214	0.0826 (7)	0.7521 (16)	0.4026 (5)	0.058 (4)
C215	0.0349 (7)	0.9462 (17)	0.3918 (6)	0.068 (4)
C216	−0.0372 (7)	0.9786 (16)	0.3285 (6)	0.064 (4)
C217	0.1637 (7)	0.7209 (19)	0.4719 (7)	0.075 (5)
C218	0.2561 (9)	0.812 (4)	0.4487 (10)	0.150 (12)
C219	0.1511 (11)	0.856 (2)	0.5422 (7)	0.108 (7)
C220	0.1658 (12)	0.482 (2)	0.5017 (9)	0.135 (9)
C221	−0.2417 (6)	0.8196 (15)	0.2371 (5)	0.045 (3)
C222	−0.2638 (7)	0.6172 (16)	0.2703 (6)	0.058 (4)
C223	−0.3454 (7)	0.5842 (16)	0.2994 (6)	0.064 (4)
C224	−0.4106 (7)	0.7469 (16)	0.2975 (5)	0.053 (4)
C225	−0.3865 (7)	0.9502 (17)	0.2638 (6)	0.066 (4)
C226	−0.3050 (7)	0.9858 (16)	0.2346 (6)	0.061 (4)
C227'	−0.4995 (7)	0.7167 (16)	0.3323 (6)	0.060 (4)
C228	−0.4821 (9)	0.844 (2)	0.4079 (7)	0.097 (7)
C229	−0.5847 (8)	0.809 (2)	0.2770 (7)	0.091 (6)
C230	−0.5228 (8)	0.473 (2)	0.3498 (8)	0.092(6)

Site occupancies: for (1*a*): C(8/8*A*) = 0.40/0.60, C(12–20/12*A*–20*A*) = 0.50/0.50, C(22–30/22*A*–30*A*) = 0.57/0.43; for (1*b*): C(8/8*A*), molecule 1 = 0.43 (3)/0.57 (3), C(18–20/18*A*–20*A*), molecule 2 = 0.74 (3)/ 0.26 (3); for (2*b*): C(8/8*A*), molecule 1 = 0.50/0.50. C(9/9*A*), molecule 2 = 0.70/0.30.

channels along the **b** axis where half the guest molecules (those labeled as 2) are included. The other half (labeled as 1) are also located in channels along **b**. They are, however, located at the interface between the crystal domains. The relative displacement of the domains along the **c** axis in (1*b*) is accompanied by a change in the orientation (see below) of the guest molecules located at the interface, giving rise to (1*a*).

In (1*b*) the two independent guests are located in two similarly shaped channels. However, the first one, which includes guest molecule (1), is approximately 0.7 Å wider along the **c** axis (Cano & Martínez-Ripoll, 1992). The orientations of the planar DMF molecules inside each channel are also different: perpendicular to the **ac** plane, 'out-of-plane' in the case of molecule (2) and more closely parallel to it, 'in-plane' for molecule (1), Fig. 3(*b*) [86.4 (14) and 39.9 (8)° are the values for the angles between the **ac** plane and those defined by the N(1), C(3) and O(6) DMF atoms, respectively]. After the phase transition, in (1*a*), there is only one independent host–guest pair and all guest molecules are perpendicularly oriented [84.0 (7)°], Fig. 2(*a*). This indicates that the DMF guest has rotated within the channel, giving rise to a more compact structure. The total packing coefficients,

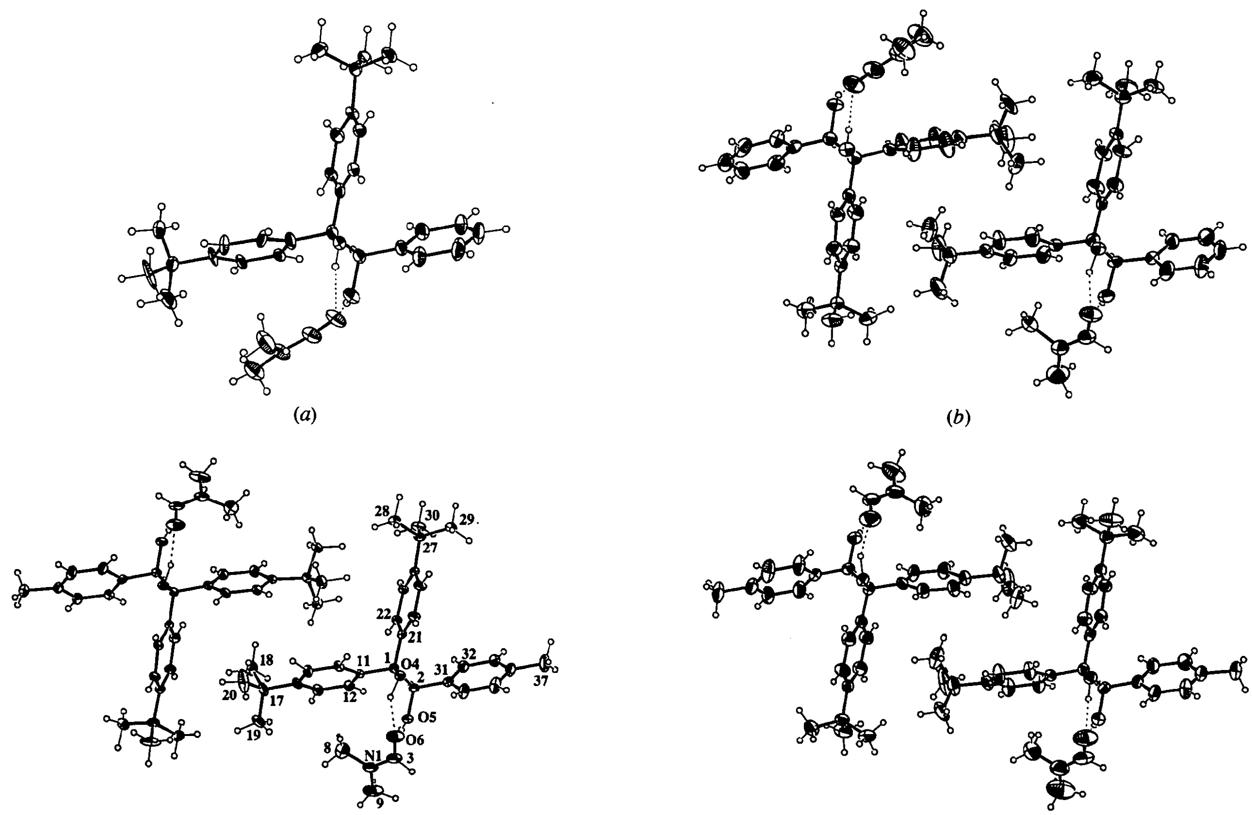

Fig. 1. A perspective view of the independent molecules of (*a*) (1*a*), low-temperature form, (*b*) (1*b*), high-temperature form, (*c*) (2*a*), low-temperature form and (*d*) (2*b*), high-temperature form, along the crystallographic **b** axes. The numbering system, analogous in all molecules, is given in (*c*). The displacement ellipsoids are drawn at the 30% probability level. Dotted lines indicate hydrogen bonds and the disorder models are omitted for clarity.

Table 3. *Selected geometrical parameters (Å,°) for the low- and high-temperature forms, respectively*

C(*i*1–*i*6) are the centroids of the corresponding rings.

	(1*a*)	(1*b*), molecule 1	(1*b*), molecule 2
C(1)—C(2)	1.551 (7)	1.525 (12)	1.561 (14)
C(1)—O(4)	1.435 (6)	1.455 (10)	1.435 (14)
C(1)—C(11)	1.546 (6)	1.549 (11)	1.506 (11)
C(1)—C(21)	1.513 (7)	1.518 (10)	1.526 (11)
C(2)—C(31)	1.513 (5)	1.518 (12)	1.495 (12)
C(2)—O(5)	1.438 (6)	1.444 (9)	1.423 (9)
C(12)—C(11)—C(16)	116.4 (9)/118.4 (9)	116.4 (11)	114.7 (11)
C(22)—C(21)—C(26)	119.8 (9)/109.2 (9)	118.0 (10)	117.0 (10)
C(32)—C(31)—C(36)	118.9 (7)	118.7 (11)	117.4 (11)
C(13)—C(14)—C(15)	117.8 (15)/115.9 (17)	115.7 (10)	114.7 (13)
C(23)—C(24)—C(25)	118.0 (15)/116.2 (21)	115.4 (10)	116.4 (11)
C(33)—C(34)—C(35)	119.7 (10)	121.8 (14)	119.9 (14)
C(2)—C(1)—C(11)	110.0 (2)	112.4 (4)	111.0 (7)
C(1)—C(11)—C(12)	121.6 (5)/120.7 (6)	123.7 (7)	125.6 (8)
C(2)—C(1)—C(21)	111.5 (2)	110.8 (4)	110.1 (6)
C(1)—C(21)—C(22)	112.7 (5)/134.3 (7)	120.1 (7)	121.3 (8)
O(4)—C(1)—C(2)—O(5)	59.1 (5)	61.2 (8)	60.6 (9)
C(21)—C(1)—C(2)—C(31)	54.6 (6)	57.7 (9)	55.6 (10)
C(11)—C(1)—C(2)—C(31)	176.7 (4)	−179.3 (7)	177.5 (8)
C(1)—C(2)—C(31)—C(32)	−116.4 (6)	−108.1 (10)	−114.8 (10)
C(2)—C(1)—C(11)—C(12)	−23.8 (7)/−70.0 (8)	−28.8 (11)	−35.5 (13)
C(2)—C(1)—C(21)—C(22)	64.6 (7)/27.9 (11)	68.2 (10)	64.4 (11)
N(1)—C(3)—O(6)···O(4)	−126.4 (7)	−86.3 (15)	−132.4 (13)
C(3)—O(6)···O(4)—C(1)	−29.2 (6)	10.3 (12)	−21.5 (12)
O(6)···O(4)—C(1)—C(2)	−57.7 (5)	−57.6 (8)	−65.6 (9)

Hydrogen interactions	*X*—H	H···*X*	*X*···*Y*	*X*—H···*Y*
(1*a*)				
O(4)—H(4)···O(6)	0.84	2.21	2.968 (6)	151
O(5)—H(5)···O(6)[i]	0.86	1.94	2.804 (9)	179
C(12)—H(12)···O(6)[i]	1.00	2.60	3.374 (11)	134
C(3)—H(3)···O(5)	0.95	2.61	3.374 (9)	137
C(8)—H(8a)···C(11–16)[ii]	0.92	2.70	3.577 (35)	158
(1*b*), molecule 1				
O(4)—H(4)···O(6)	1.03	2.19	2.980 (11)	132
O(5)—H(5)···O(6)[i]	0.82	2.02	2.838 (15)	176
C(3)—H(3)···O(5)[iii]	1.01	2.68	3.450 (12)	134
C(8)—H(8a)···C(11–16)	1.00	2.70	3.562 (38)	144
(1*b*), molecule 2				
O(4)—H(4)···O(6)	0.79	2.36	2.935 (10)	130
O(5)—H(5)···O(6)[i]	0.69	2.24	2.893 (15)	158
C(3)—H(3)···O(5)	1.01	2.59	3.403 (17)	137

	(2*a*), molecule 1	(2*a*), molecule 2	(2*b*), molecule 1	(2*b*), molecule 2
C(1)—C(2)	1.549 (6)	1.544 (7)	1.540 (9)	1.552 (13)
C(1)—O(4)	1.424 (6)	1.434 (8)	1.451 (8)	1.439 (12)
C(1)—C(11)	1.549 (6)	1.542 (5)	1.530 (8)	1.548 (12)
C(1)—C(21)	1.522 (5)	1.520 (5)	1.520 (10)	1.511 (14)
C(2)—C(31)	1.524 (6)	1.531 (6)	1.513 (12)	1.504 (12)
C(2)—O(5)	1.439 (5)	1.422 (5)	1.431 (13)	1.427 (13)
C(12)—C(11)—C(16)	118.1 (5)	117.4 (5)	116.6 (9)	117.7 (9)
C(22)—C(21)—C(26)	118.2 (5)	117.6 (5)	116.4 (8)	117.4 (8)
C(32)—C(31)—C(36)	119.0 (6)	118.4 (5)	118.3 (9)	117.6 (10)
C(13)—C(14)—C(15)	117.3 (6)	116.7 (6)	115.9 (10)	116.8 (9)
C(23)—C(24)—C(25)	117.3 (6)	116.3 (5)	116.4 (8)	114.8 (9)
C(33)—C(34)—C(35)	117.4 (7)	118.1 (6)	119.0 (12)	116.4 (14)
C(2)—C(1)—C(11)	111.8 (2)	112.1 (3)	111.5 (5)	111.8 (7)
C(1)—C(11)—C(12)	123.0 (4)	123.9 (4)	123.9 (8)	123.2 (8)

Table 3 (*cont.*)

	(2*a*), molecule 1	(2*a*), molecule 2	(2*b*), molecule 1	(2*b*), molecule 2
C(2)—C(1)—C(21)	109.7 (2)	110.5 (3)	111.6 (5)	111.0 (7)
C(1)—C(21)—C(22)	119.8 (3)	120.7 (4)	120.1 (8)	120.6 (8)
O(4)—C(1)—C(2)—O(5)	58.3 (4)	61.2 (5)	58.4 (7)	56.6 (9)
C(21)—C(1)—C(2)—C(31)	54.1 (5)	57.6 (5)	53.7 (8)	53.6 (10)
C(11)—C(1)—C(2)—C(31)	175.6 (4)	177.5 (4)	175.4 (7)	176.0 (8)
C(1)—C(2)—C(31)—C(32)	−108.5 (5)	−108.0 (5)	−108.8 (10)	−109.5 (10)
C(2)—C(1)—C(11)—C(12)	−22.0 (6)	−24.6 (7)	−27.8 (11)	−24.1 (12)
C(2)—C(1)—C(21)—C(22)	64.7 (5)	55.3 (6)	64.4 (9)	65.6 (11)
N(1)—C(3)—O(6)···O(4)	−79.7 (7)	−95.8 (7)	−87.5 (17)	−81.6 (14)
C(3)—O(6)···O(4)—C(1)	16.3 (6)	31.0 (6)	16.7 (13)	19.4 (13)
O(6)···O(4)—C(1)—C(2)	−57.5 (4)	−69.9 (4)	−60.5 (7)	−60.1 (10)

Hydrogen interactions	*X*—H	H···*X*	*X*···*Y*	*X*—H···*Y*
(2*a*), molecule 1				
O(4)—H(4)···O(6)	1.06 (5)	2.11 (6)	3.000 (6)	140 (5)
O(5)—H(5)···O(6)^{i}	0.91 (7)	1.93 (8)	2.788 (8)	156 (5)
C(8)—H(8a)···C(11–16)	0.95	2.84	3.703 (10)	152
C(9)—H(9b)···C(31–36)^{iv}	0.93 (9)	3.03 (10)	3.653 (9)	125 (8)
(2*a*), molecule 2				
O(4)—H(4)···O(6)	0.96 (5)	2.08 (6)	2.995 (5)	157 (5)
O(5)—H(5)···O(6)^{i}	0.94 (7)	1.89 (8)	2.773 (8)	154 (6)
C(8)—H(8a)···C(11–16)	1.17 (14)	2.63 (13)	3.659 (10)	145 (9)
C(9)—H(9b)···C(31–36)^{v}	0.96 (7)	2.94 (8)	3.526 (8)	121 (6)
(2*b*), molecule 1				
O(4)—H(4)···O(6)	0.96	2.14	2.998 (16)	149
O(5)—H(5)···O(6)^{i}	0.85	1.95	2.800 (14)	178
C(8)—H(8a)···C(11–16)	1.11	2.81	3.717 (49)	139
C(9)—H(9b)···C(31–36)^{vi}, molecule 2	0.92	3.06	3.691 (25)	128
(2b), molecule 2				
O(4)—H(4)···O(6)	1.04	2.13	3.031 (14)	143
O(5)—H(5)···O(6)^{i}	0.81	2.02	2.833 (14)	177
C(9)—H(9b)···C(31–36)^{vii}, molecule 1	0.96	3.01	3.708 (25)	130

Symmetry codes: (i) $x, y-1, z$; (ii) $x, y+1, z$; (iii) $-x, \frac{1}{2}+y, 1-z$; (iv) $1-x, \frac{1}{2}+y, 1-z$; (v) $1-x, \frac{1}{2}+y, -z$; (vi) $x, y, 1+z$; (vii) $x, 1+y, 1-z$.

calculated as $V_{\text{molecules}}/V_{\text{unit cell}}$, and using as van der Waals radii those reported in Vainshtein *et al.* (1982), are 0.66 and 0.64 for (1*a*) and (1*b*), respectively.

In both forms, almost all hydrogen-bond interactions, reported in Table 3, are between host–guest pairs to give the previously described chains of molecules along the **b** axis. The only exception is the weak C(3)—H(3)···O(5) interaction which appears after the orientation change of the guest molecule, molecule 1 in form (1*b*), and interconnects two chains of molecules related by a twofold screw axis.

3.4. *Structural comparison between the forms of (2)*

In the packing arrangement of (2*b*), a pseudo-twofold screw axis passing through the origin and approximately parallel to **b** again relates the two independent host molecules [x = −0.006 (2), z = −0.005 (2) with a translation of −0.45 (3), χ^2 for x, y and z coordinates = 9.5, 1.2 and 10.5 *versus* 33.9 (Nardelli, 1983); Fig. 3*d*]. Therefore, the crystal packing of (2*b*) can be described as having a pseudo-$P2_1$ space group, with one host–guest pair in the crystallographic asymmetric unit. Then, the symmetry changes caused by the phase transition become analogous to that described for (1). The unit cell of (2*b*) (**a**′, **b**′, **c**′) can be obtained from that of (2*a*) (**a**, **b**, **c**) according to the transformation **a**′ = $\frac{1}{2}$(**a** + **c**), **b**′ = **b**, **c**′ = $\frac{1}{2}$(−**a** + **c**) and an origin shift of ($\frac{1}{2}$, 0, 0) (calculated values of 14.219, 5.952, 17.487 Å; 90, 100.3, 90°), which are similar to the values reported in Table 1, the given transformation again being from the higher symmetry to the lower one.

The phase transition from (2*b*) to (2*a*) can also be described as a displacive movement (McCrone, 1965) of layers of molecules, parallel to the diagonal **ac**, **b** plane [**ab** plane in (2*a*)] along the **b** axis. Within the layer this leads to higher symmetry by the reorganization of the molecules along the shortest **b** axis; that is, the molecules within the layer are related by a pseudo-2_1 axis in (2*b*) *versus* a crystallographic 2_1 one in (2*a*) (see below). Moreover, between layers, in (2*a*) the crystal is built up of different independent molecules almost related by a binary axis at approximately $x = 0.253$ (1), $z = 0.250$ (4) with a translation along **b** of 0.27 (6) (χ^2 for x, y and z coordinates = 47.1, 2.3, 22.7 for a tabulated value of 27.6). In this case, form (2*a*), the phenyl ring atoms C(22)–C(26) have been omitted from the comparison between both independent molecules due to the significant differences in the torsion angle of this ring, Table 3, while in (2*b*) the structurally equivalent layers are formed by the two independent molecules and they are related by the pseudo-2_1 axis. The guest molecules are placed analogously with respect to the host in both forms, although they are nearer to the host in (2*a*) (Table 3) and the whole structure appears to be contracted, probably due to the effect of decreasing the temperature. This can also be seen in the values of the total packing coefficients ($V_{\rm molecules}/V_{\rm unit\ cell}$): 0.65 and 0.62 for (2*a*) and (2*b*), respectively.

In both cases, the chains of hydrogen-bonded host–guest molecules are joined in pairs through (Me)C—H$\cdots\pi$ electron cloud(Ph) hydrogen interactions, Table 3. In (2*a*) the pairs are formed by two twofold screw-related chains and in (2*b*) they are formed by two pseudo-twofold screw-related ones, *i.e.* both crystallographically independent host–guest pairs are involved in these structural motifs.

3.5. *General considerations*

Although the structural changes related to the phase transition (considering only symmetry or pseudo-symmetry relationships) are equivalent in both pairs of host–guest complexes, the changes in the crystal arrangement of molecules in the phase transition of (2) are different to those found in that of (1). Form (2*b*) (pseudo-$P2_1$) is structurally equivalent to (1*a*) ($P2_1$), Figs. 3(*a*) and 3(*d*). The main difference is the expansion of the host network in (2*b*) induced by the presence of the methyl group at the *para* position of the C(31–36) phenyl ring. This enlargement of the host network produces wider channels where the guest molecules adopt an 'in-plane' orientation, rather than the 'out-of-plane' one displayed in (1*a*). The 'in-plane' orientation of the guest is also maintained in (2*a*) and (2*b*) [41.5 (4), 47.3 (3)° and 46.1 (7), 40.9 (4)° are the values for the angles between the **ac** plane and those defined by the N(1), C(3) and O(6) DMF atoms in (2*a*) and (2*b*), respectively], where the host channels are of very similar size. A further temperature-induced contraction in (2*a*) is prohibited by the methyl groups of C(31–36), which enlarge the **c** axis in (2*a*) with respect to (1*b*). Therefore, the DMF guest remains in the 'in-plane' position. With no methyl groups, this steric hindrance does not exist and there is a possibility of additional contraction, as happens from (1*b*) to (1*a*). So, at high temperature, one pair of the DMF guest molecules is in the 'out-of-plane' position and further cooling leads to the flip of the remaining 'in-plane' pair of guest molecules in the unit cell and causes the appearance of another set of 2_1 symmetry elements. This results in a half-volume unit cell with a content of only two host–guest pairs. The influence of the methyl group results in an elongation of the **c** axis by approximately 1.5 Å, similar to the value found when comparing (1*b*) and (2*a*) (Figs. 3*b* and 3*c*), taking into account the effect of dilatation due to the temperature.

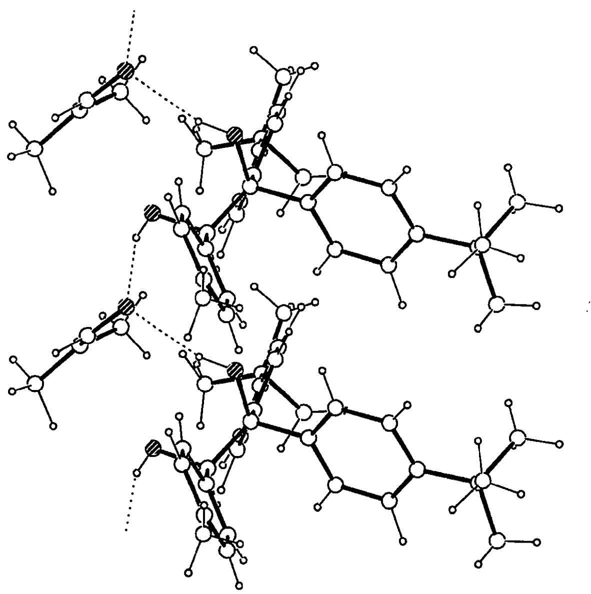

Fig. 2. A chain of O—H$\cdots$O hydrogen-bonded host and guest molecules of (2*a*) (molecule 1) parallel to the crystallographic **b** axis. Atoms are shown as spheres of arbitrary size to minimize overlapping and the O atoms have been shaded.

4. Conclusions

The influence of the substituents on the phenyl groups does not affect the overall crystal packing modes in this class of mandelic acid-derived hosts. The methyl group at the *para* position [R^1 in (I)] seems to influence directly only the manner of the phase transition and the temperature at which the transition occurs. Another interesting observation is that this behavior can only be found with DMF as the guest molecule; in the analogous cases of dimethylsulfoxide (DMSO) inclusions no phase transition could be found; this might be due to the form and size of the cavities in which the guest is accommodated or to the electronic and steric properties of the DMF guest. These two systems have two well defined situations, their phases and the systems can be moved from one situation to the other using a controllable process, namely a change in temperature. Furthermore, the actual situation can be detected unequivocally due to the different crystal lattices.

The authors gratefully acknowledge financial support from the European Community, Project No. CIPA-CT 93-0171.

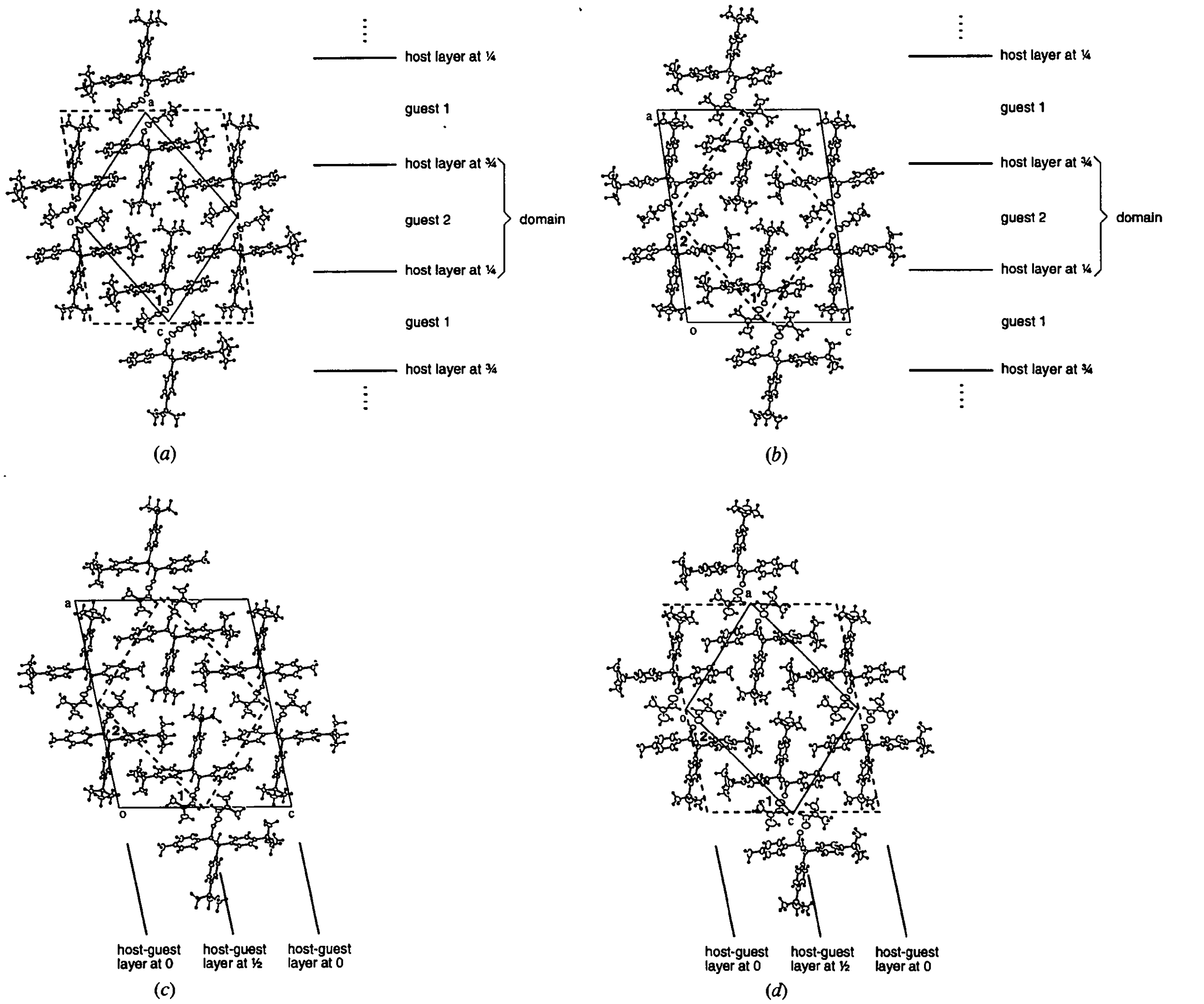

Fig. 3. Packing diagrams viewed along **b**, the shortest crystallographic axis, (*a*) for (1*a*), low-temperature form, (*b*) (1*b*), high-temperautre form, (*c*) (2*a*), low-temperature form, and (*d*) (2*b*), high-temperature form. Dashed lines represent the unit cell after phase transformation. A schematic representation of the layers of molecules used to describe the phase transformation is also given for each case.

References

Allen, F. H., Davies, J. E., Galloy, J. J., Johnson, O., Kennard, O., Macrae, C. F., Mitchell, E. M., Mitchell, G. F., Smith, J. M. & Watson, D. G. (1991). *J. Chem. Inf. Comput. Sci.* **31**, 187–204.

Altomare, A., Cascarano, G., Giacovazzo, C., Guagliardi, A., Burla, M. C., Polidori, G. & Camalli, M. (1994). *J. Appl. Cryst.* **27**, 435.

Appleman, D. E. (1984). *LSUCRE. Program for Least-Squares Refinement of Reticular Constants.* US Geological Survey, Washington DC.

Cano, F. H. & Martínez-Ripoll, M. (1992). *J. Mol. Struct. (Theochem.)* **258**, 139–158.

Cosier, J. & Glazer, A. M. (1986). *J. Appl. Cryst.* **19**, 105–107.

Dunitz, J. D. (1995). *Acta Cryst.* **B51**, 619–631.

Domenicano, A. & Murray-Rust, P. (1979). *Tetrahedron Lett.* **24**, 2283–2288.

Hall, S. R., Flack, H. D. & Stewart, J. M. (1994). Editors. *Xtal*3.2 *User's Manual.* University of Western Australia, Australia.

Martínez-Ripoll, M. & Cano, F. H. (1975). *PESOS. Program to Analyse and Establish Weighting Schemes for Structure Refinement.* Departamento de Cristalografía, Instituto de Rocasolano, CSIC, Madrid.

McCrone, W. C. (1965). *Physics and Chemistry of the Organic Solid State*, edited by D. Fox, M. M. Labes & A. Weissenberger, Vol. 2, pp. 735–767. New York: Interscience.

Nardelli, M. (1983). *Comput. Chem.* **7**, 95–98.

Vainshtein, B. K., Fridkin, V. M. & Indenbom, V. L. (1982). *Modern Crystallography II*, p. 87. Berlin, Heidelberg, New York: Springer-Verlag.

Weber, E., Hager, O., Foces-Foces, C. & Llamas-Saiz, A. L. (1996). *J. Phys. Org. Chem.* **9**, 50–60.

Weber, E., Hager, O., Foces-Foces, C. & Llamas-Saiz, A. L. (1998*a*). *Supramol. Chem.* In the press.

Weber, E., Hager, O., Foces-Foces, C. & Llamas-Saiz, A. L. (1998*b*). *J. Incl. Phenom.* Submitted.
Weber, E. & Wimmer, C. (1993). *Chirality*, **5**, 315–319.
Weber, E., Wimmer, C., Llamas-Saiz, A. L. & Foces-Foces, C. (1992). *J. Chem. Soc. Chem. Commun.* pp. 733–735.
Zachariasen, W. H. (1968). *Acta Cryst.* A**24**, 212–216.